Atmos. Meas. Tech. Discuss., doi:10.5194/amt-2016-67, 2016
Manuscript under review for journal Atmos. Meas. Tech.
Published: 8 March 2016

Atmospheric Measurement Techniques Discussions

Application of Oxygen A-band Equivalent Width for Cloud Optical Depth Measurement

Edward R. Niple[1], Herman E. Scott[1], John A. Conant[1], Stephen H. Jones[1], Frank J. Iannarilli[1], and Wellesley E. Pereira[2]

[1]{Aerodyne Research, Inc., Billerica, MA, USA}

[2]{Air Force Research Lab, Albuquerque, NM, USA}

Correspondence to: F. J. Iannarilli (franki@aerodyne.com)

Abstract

This paper presents a new technique for measuring Cloud Optical Depth (COD). It is based on ground-based visible band zenith spectral radiances much like the AERONET Cloud-Mode sensors. What is novel in our approach is that we employ absorption in the oxygen A-band as a means of resolving the COD Ambiguity inherent in using up-looking spectral radiances. We describe the algorithm and a sensor that implements it, and compare its performance to AERONET Cloud-Mode measurements collected during the Two Column Aerosol Project (TCAP). Spectral radiance agreement was excellent (better than 1%) while COD agreement was good.

Keywords

Cloud optical depth, radiative transfer, oxygen A-band, liquid water path, equivalent width

1 Introduction

Accurate global climate model (GCM) predictions are absolutely essential. Not only are they needed to help mitigate damage from unwanted climate changes, but also to determine what, if any, interventions can reverse those changes directly. Yet clouds, because of their complexity and inherently random nature, have always been one of the primary obstacles to GCM accuracy. The work reported here is intended to help this situation by improving cloud

Atmos. Meas. Tech. Discuss., doi:10.5194/amt-2016-67, 2016
Manuscript under review for journal Atmos. Meas. Tech.
Published: 8 March 2016

Atmospheric Measurement Techniques Discussions

radiative property measurements, in particular, cloud optical depth, the most fundamental cloud radiative property.

2 Principle of Operation

The general measurement consists of a zenith staring spectral radiometer recording the absolute power coming from a narrow field of view (FOV) in a collection of spectral bands. Assuming the sensor's FOV does not include the sun, this consists of solar radiation scattered by the molecules, aerosols, and cloud droplets in the FOV, which may include radiation that has been scattered multiple times from the atmosphere and the terrain. The visible spectral band (Figure 1), at a moderate spectral resolution of 2 nm shows a broad baseline with multiple narrow absorption features. Many of these are due to water vapor, as well as constituents of the sun, but one particular feature at 760 nm is the well-known O_2 A-band. This feature is free from absorption by other atmospheric constituents and provides a direct measurement of the average amount of oxygen-density-weighted photon path length from the sun to the sensor. Since oxygen is uniformly mixed in the atmosphere, this is related to the photon's physical path length.

Our algorithm uses three spectral factors: the spectral radiances at 440 nm and 870 nm (SR440 and SR870) and the equivalent width of the oxygen A-band (EQW). The equivalent width is computed from the spectral radiances between 750 to 785 nm by fitting a straight line to the baseline from 750 - 760 nm and 770 - 785 nm, dividing each measured spectral radiance by the corresponding linear fit baseline to produce a transmittance value, and then integrating the area under the absorption band. This requires an accurate determination of the zero radiance level. The spectral radiances at 440 nm and 870 nm are in regions relatively free from atmospheric absorption. These three factors are then used to determine the COD: all three to determine cloud state (thick, thin, or blue sky), and SR440 for numerical COD by comparison to model predictions. The model used is MODTRAN5 (Berk et al., 2006) for a typical water stratus cloud over a range of COD and solar zenith angles.

3 Prior Art

The use of zenith spectral radiances to measure COD began with the work of Marshak et al, (2004) using a technique first suggested by Marshak et al, (2000) and Barker and Marshak, (2001). In order to resolve the COD ambiguity they use spectral radiances at red (670 nm) and NIR (870 nm) wavelengths which sit on opposite sides of the chlorophyll red edge feature of the albedo of vegetated terrain. The technique was validated at the ARM site in Oklahoma

Atmos. Meas. Tech. Discuss., doi:10.5194/amt-2016-67, 2016
Manuscript under review for journal Atmos. Meas. Tech.
Published: 8 March 2016

by comparison to more conventional techniques (Microwave Radiometer and Multifilter Rotating Shadowband Radiometer). In the work of Chiu et al, (2006) the preliminary validation was extended. In Chiu et al, (2010) the technique was improved by switching to blue (440 nm) and NIR (870 nm) wavelengths.

The oxygen A-band at 760 nm, already referred to as "the well-known atmospheric band system" by Mulliken, (1928) when he first published the interpretation of the bands, has been used for many years to study the atmosphere from satellite and ground-based sensors. Wark and Mercer, (1965) first proposed using the A-band to study cloud top heights from space and Pfeilsticker et al, (1998) first used the A-band to study the probability density function of geometrical path lengths for skylight transmitted from clear and cloudy skies to the ground, following the suggestion of Pfeilsticker et al, (1996) and Harrison and Min, (1997). Our technique is merely one more application of the A-band; in this case, to help determine COD.

4 "Nose" Plot

COD is a two-valued function of up-looking spectral radiance while oxygen equivalent width is a monotonic function of COD, so the EQW supplies useful information about whether a measurement is in the optically-thin or optically-thick regimes. By plotting SR440 versus EQW as COD increases from no cloud to thick clouds one traces out a "nose-like" shape (Figure 2). The lower portion of the "nose" where the slope is positive corresponds to the optically thin state; the upper portion corresponds to the optically thick state. Within a span of several seconds, real clouds do not trace out a complete nose but only a small segment of it as the cloud evolves and drifts in the wind over the sensor. Whether the cloud changes involve increases or decreases of the COD, the slope of the corresponding segment indicates the cloud's optical state. This is the basis for the new algorithm as it allows us to resolve the COD ambiguity.

5 The New Three Waveband Spectrally-agile Technique (TWST) Algorithm

Our new algorithm involves two steps. The first is to determine the optical state of the cloud. We do this in two different regimes. When the COD is very low, the amount of radiation in the NIR is very small and the signal to noise ratio of the equivalent width and thus the nose plot slope is too low to resolve the state. The ratio of SR440 to SR870, which we call the Blueness factor, has a much higher SNR and is more reliable. This, of course, is a simple consequence of the wavelength dependence of Rayleigh scattering. We have found a threshold of 5 is a sure indicator of optically thin clouds. When the Blueness factor is less

Atmos. Meas. Tech. Discuss., doi:10.5194/amt-2016-67, 2016
Manuscript under review for journal Atmos. Meas. Tech.
Published: 8 March 2016

Atmospheric Measurement Techniques Discussions

than 2, the cloud's optical state is not well correlated with the Blueness factor, and we must rely on the nose plot slope.

If measured nose plots were as pristine as indicated in Figure 2, the determination of state would be nearly trivial. A linear regression over a short time segment would suffice. However, measured nose plots deviate from the ideal due largely to time varying structure in the field-of-view but also to temporal variation of the "bright point" (the "nose tip"). Figure 3 shows a typical nose plot for over 13 hours of data with a 10 minute segment highlighted. In the top plot, it is not too difficult to see that the 10 minute segment lies in a positive slope region and thus is indicative of an optically thin cloud. However, this assessment takes into account a great deal of context that is not evident if the 10 minute segment is examined by itself as can be seen in the bottom part of the figure. Clearly, a simple linear regression would yield highly erroneous results. It should be noted here that the signal to noise ratio of the measurements is very high, often >1000. Consequently, increased integration time will not improve the situation.

The qualitative reduction in ambiguity afforded by examining the much larger time record suggests the use of a filter with memory. For example, we know that clouds do not switch rapidly between the thick and thin states except possibly near the bright point where the switch is inconsequential anyhow. We implemented a time varying hysteresis filter to effectively avoid this unwanted switching. The hysteresis action is achieved by keeping track of the maximum and minimum values of equivalent width over a predetermined time interval, typically about three minutes. In order to drive the filter toward a different state, the hysteresis limits must be exceeded. The output of the hysteresis filter is discrete ternary: -1, 0 or 1, corresponding to thick, indeterminate or thin. Finally, this ternary variable is input to a linear, single pole autoregressive (AR(1)) filter to afford additional smoothing. The output of this filter is thresholded and used as the state estimate.

Once the cloud's optical state is determined, the COD is obtained from a table of MODTRAN5 computations of SR440 at a grid of COD and solar zenith angles. Various table lookup algorithms were investigated. A reasonable tradeoff between accuracy and speed is a combination of 1-D spline interpolations and searching for the tabulated solar zenith angle (SZA) closest to the current solar zenith angle based on the current time, day of the year and latitude/longitude of the sensor. The first step involves preprocessing the MODTRAN5 results to find the COD (CODmax) of the brightest SR440 (SR440max) for each SZA. These are

Atmos. Meas. Tech. Discuss., doi:10.5194/amt-2016-67, 2016
Manuscript under review for journal Atmos. Meas. Tech.
Published: 8 March 2016

Atmospheric Measurement Techniques Discussions

then used to compute spline coefficients for SR440max as a function of SZA. Spline coefficients are then computed for both optical states for each COD as a function of SR440. All these spline coefficients are computed once the MODTRAN5 data is generated and then stored for use during instrument operation.

During operation, the measured spectral radiance $L_{obs}(\theta_{obs})$ at 440 nm is scaled to a corresponding L_{sc} at the tabulated solar zenith angle θ_{table} nearest the current solar zenith angle θ_{obs} according to

$$L_{sc} = \frac{L_{obs}(\theta_{obs})\, L_{table}(\theta_{table})}{L_{max}(\theta_{obs})}, \quad (1)$$

where $L_{table}(\theta_{table})$ is the tabulated spectral radiance and $L_{max}(\theta_{obs})$ is the interpolated maximum spectral radiance at the current solar zenith angle. The corresponding COD is then computed by spline interpolation of L_{sc}.

At this point it is important to note that the spectral radiance chosen at some other wavelength than 440 nm could be used for the radiance-to-COD look-up. We chose 440 nm for this effort because that is a wavelength used by AERONET Cloud-Mode sensors, which serve as a source for comparative validation. In principle the choice of wavelength depends on the ground albedo of the measurement site. One wants a wavelength with the lowest absolute albedo uncertainty to minimize errors in the COD due to errors in the assumed albedo for the MODTRAN5 computations. This flexibility in our algorithm is what gives our approach spectral agility

6 Sensitivity Studies

The TWST algorithm currently operates without any information on the droplet size distribution or the cloud base height, and with a prior estimate of the ground albedo. We performed some initial sensitivity studies on these parameters.

Water cloud drop-size distributions typically vary from an effective radius of 1 – 20 μm (see e.g. Chiu et al, (2006)). Because our implementation of the TWST algorithm uses a radiance database generated with the MODTRAN model, we studied 440 nm radiances from four different cloud types included with MODTRAN. These types have effective radii of 12.0 (cumulus), 7.2 (altostratus), 8.3 (stratus), and 6.7 (stratocumulus) μm. We modeled clouds with fixed base height of 0.5 km and fixed physical thickness of 0.5 km. For each cloud type we varied the Liquid Water Path (LWP) enough to achieve 550 nm CODs between 0 and 100;

Atmos. Meas. Tech. Discuss., doi:10.5194/amt-2016-67, 2016
Manuscript under review for journal Atmos. Meas. Tech.
Published: 8 March 2016

Atmospheric Measurement Techniques Discussions

LWP was used because it is an input to MODTRAN. COD values were estimated from LWP using the Wood and Hartmann, (2006) modification to the Stephens, (1978) formula as described in Chiu et al, (2012). Figure 4 shows the computed 440 nm vertical radiances plotted versus LWP and COD. The different size distributions lead to different radiances for the same LWP as expected. However, in the COD vs. radiance plot the curves overlay closely. We verified this intuitive result using a simple two-stream computation as an alternative to the DISORT algorithm included within MODTRAN (Stamnes et al, 1988). This relation gives us some confidence in reporting COD values from radiances at the non-absorbing 440 nm wavelength.

Inter-reflections between the ground and a thick cloud can be significant unless the Earth albedo is low. The TWST algorithm uses a look-up table of radiance computations for 440 nm. At that wavelength most Earth cover types have albedo of 0.2 or less as shown in Figure 5 with samples of the ASTER Database (Baldridge et al, 2009); notable exceptions are for white sand, fresh snow, and ocean ice. To characterize the sensitivity of retrieved COD due to albedo variability, we used MODTRAN to compute 440 nm zenith radiances for albedos of 0.0, 0.1, 0.2 and 0.5, over a range of solar zeniths and cloud thicknesses. Figure 6 presents a first-order indication of sensitivity, and plots 440 nm radiances versus COD for albedo bounds of 0.0 and 0.5. The thin/thick duality, the strong variation with solar zenith, and the weaker variation with ground albedo are evident in these plotted results.

The plot in Figure 7 shows the absolute change in retrieved COD for an unexpected increase in the ground albedo from 0.1 to 0.2. Each curve, plotted versus SZA, is for a different percentage of the bright point radiance "Lbrt" (which varies with SZA), for either thick or thin cloud. For any solar zenith angle, there is a "bright point" where the cloud radiance is a maximum, typically occurring for a COD between 2 and 8, as seen in Figure 6. Note that we used *linear* interpolations of our data table in computing the CODs for this study, but near the bright point (red curves in Figure 7) the COD vs radiance is quite non-linear, and thus the red curves are less-precise, and jagged. (The TWST retrieval algorithm doesn't suffer this limitation, as it employs *non-linear* spline interpolation). These curves show that a higher than expected albedo implies retrieval of a higher (lower) COD in the Thick (Thin) region. This is because an elevated albedo increases the cloud radiance, but decreases its percent brightness relative to the higher bright point radiance (Figure 6). The largest change we found

Atmos. Meas. Tech. Discuss., doi:10.5194/amt-2016-67, 2016
Manuscript under review for journal Atmos. Meas. Tech.
Published: 8 March 2016

was ΔCOD of 5, but that occurred for very thick clouds, such that the relative change was only 10%.

For low-altitude water clouds, uncertainty in the cloud base height has a negligible impact on COD retrieval. We ran MODTRAN for cloud base heights of 500 m and 2 km, iterating over 10 COD and 11 solar zeniths for each. The 440 nm radiances were nearly identical, as shown in the scatter plot of Figure 8.

7 The TWST Sensor

The heart of the TWST sensor is a zenith-pointing calibrated spectroradiometer. We elected to design the sensor around a commercial compact grating spectrometer (CGS), given the significant advances in miniaturization, rugged monolithic construction, and linear array detectors. Several advantages accrue from this design choice, the most important to our COD measurement application being the acquisition of spectral radiances at high signal-to-noise-ratio (SNR) and high temporal resolution, attributed to the multiplex advantage provided by the CGS.

We have now built and tested a few different configurations of the TWST sensor, but each includes the basic elements represented in the schematic design in Figure 9; a companion photograph looking inside a recent model is shown in Figure 10. The entrance window (A) is slanted to shed rain drops. A simple mechanical shutter (S) for recording dark spectra, selected for its reliability and effective light blocking performance, is located just inside the input window and driven by an inexpensive stepping motor. An incoming light baffle (B) limits the total field-of-view (TFOV) to 0.5° FWHM. At the end of the baffle sits a 400 nm long pass filter. A collecting lens (C) then focuses the filtered light onto the end of a 400 μm dia. optical fiber (D) which feeds the light into the CGS (E). The entire system is contained in an IP66 (NEMA 4X) rated sealed enclosure with desiccant to prevent water condensation over deployment periods of several months.

The key specifications for the TWST COD sensor are listed in Table 1. Here we are excluding extreme ambient conditions outside the range of -10 C to +40 C that require special temperature control. Our design has proven to be field-worthy, easily transportable, and stable over a wide range of environmental conditions. We have experienced no instances of condensation inside the sealed TWST enclosure while operating in humidity and temperature conditions well below the dew point. The spectral resolution defined by the spectrometer configuration is currently ~2.5 nm. The temporal resolution determined by the available

Atmos. Meas. Tech. Discuss., doi:10.5194/amt-2016-67, 2016
Manuscript under review for journal Atmos. Meas. Tech.
Published: 8 March 2016

sunlight, spectrometer throughput, and linear FPA detector characteristics is a variable sampling interval from 1 msec to 60 sec (1 sec typical).

The relative precision of the TWST COD measurements determined from field data is estimated as follows. Each raw TWST spectrum consists of 400 co-added scans each of 2.5 msec integration time. The SNR for a single scan is limited to 400:1 due to photon noise based on the electron well depth of 160,000. When readout noise is included, this drops to 275:1. With 400 co-adds, the 1 second SNR is therefore limited to 5,500:1. This is the relative precision of TWST COD results. Even higher precision can be achieved by combining the 125 independent spectral channels in the 425 – 475 nm blue spectral band. This yields a potential SNR of 60,000:1 for each 1 second spectral radiance value. In terms of COD SNR, for the optically thin state, the COD ranges from 0 to about 6 in an approximately linear relationship. This implies a theoretical noise-limited sensitivity of 6/60,000 or OD of 0.0001.

8 The Two Column Aerosol Project (TCAP)

TCAP was a one year measurement campaign directed by the Atmospheric Radiation Measurements (ARM) division of the U.S. Department of Energy. It was designed to quantify aerosol properties, radiation, and cloud characteristics, producing a database to assist climate modeling studies. The ground-based campaign involved the ARM Mobile Facility (AMF) suite of sensors deployed at the ARM Highlands in Cape Cod Massachusetts. The aerial campaign involved two aircraft loaded with remote and in situ sensors. Measurements were performed from July 2012 until June 2013.

With the kind permission and assistance of the TCAP project, the TWST sensor was set up on Cape Cod near the AERONET Cloud-Mode sensor and Total Sky Imager (TSI) which are part of AMF on 17 May 2013. Data were collected continuously for a period six days. Some minor adjustments were then made to the sensor configuration, and then data were collected for the next thirty days until 27 June when the AMF was taken down in preparation for its next deployment. During this period about 50,000 spectra were collected by TWST every day at one second intervals during the day.

8.1 AERONET Cloud-Mode and TWST Data Comparison

During the time TWST was deployed on Cape Cod, AERONET collected 266 COD values that overlapped TWST measurements. In addition, 8,609 overlapping spectral radiance values

Atmos. Meas. Tech. Discuss., doi:10.5194/amt-2016-67, 2016
Manuscript under review for journal Atmos. Meas. Tech.
Published: 8 March 2016

at 440 nm were collected. Since all TWST's COD values were based on SR440 measurements, it is important to compare the SR440 values before comparing the COD values.

8.1.1 Spectral Radiance Comparison

This required careful time synchronization between the AERONET and TWST data times. A linear drift of 0.27 seconds/day was determined by least squares fits to the individual days with a 4 second difference between the high gain (x8) A and low gain (x1) K measurements from AERONET. The result (Figure 11) shows that both sensors were reporting SR440 values in very good agreement. The rms difference was 0.63 ($\mu W\ cm^{-2}\ sr^{-1}\ nm^{-1}$). A simple linear fit without constant yielded a slope of 1.003 (0.0004). TWST values at high spectral radiance showed some evidence of nonlinear response.

Several conclusions follow from the very good agreement among TWST and AERONET spectral radiances. The first is the expectation of a COD comparison not influenced by TWST spectral radiance errors. The second is the radiometric stability of TWST during its TCAP deployment. Similarly such close agreement over many different cloud conditions implies that the different fields of view (1.2 ° for AERONET versus 0.5 ° for TWST) and zenith pointing (robotic control for AERONET versus fixed tripod with bubble level for TWST) were not significantly different. Of course, the agreement only proves consistency, not accuracy for either sensor.

8.1.2 COD Comparison

The comparison of the average COD (Figure 12) shows evidence of the two different types of errors in the TWST and AERONET Cloud-Mode algorithms: errors in cloud state and errors in COD. For this comparison only the 90 second average COD was available for AERONET Cloud-Mode, which is a form of trimmed mean based on up to ten instantaneous COD measurements during each measurement period. Since TWST produces 90 instantaneous COD measurements during the same 90 second period, the trimmed mean process will have different statistical properties.

Of the 244 overlapping COD values, 235 (96%) showed the same cloud state. Some analysis was done in an effort to determine whether TWST or AERONET Cloud-Mode was probably correct. For the nine cases where AERONET and TWST disagreed on the cloud state, detailed

Atmos. Meas. Tech. Discuss., doi:10.5194/amt-2016-67, 2016
Manuscript under review for journal Atmos. Meas. Tech.
Published: 8 March 2016

nose plots were generated to see if we could visually extract more than the simple slope information used in the automated algorithm. Four of the cases produced close to the ideal nose shape, indicating that the TWST cloud state was probably correct. For the other five cases, the nose plot was too distorted to determine the cloud state, indicating that the TWST cloud state was probably incorrect and should have been assigned the "unknown" state. A linear fit of TWST to AERONET Cloud-Mode COD for the 235 cases of cloud state agreement found an average bias of 0.843 for TWST with an rms difference of OD 3.2. Although relatively few optically thin COD cases were available due to the secondary mission status of Cloud-Mode, no evidence of a constant offset between TWST and AERONET Cloud-Mode was found.

The two primary candidates for causing the observed disagreements are differences in the TWST and AERONET Cloud-Mode lookup tables and effects from the trimmed mean process. There may also be some residual effects due to FOV and pointing differences, although these are not expected to be large due to the very good spectral radiance agreement.

It must always be kept in mind that the COD values determined by TWST and AERONET Cloud-Mode are only equivalent 1D cloud quantities. Violations of 1D assumptions are present in nearly all our measurements to some extent. This includes (1) cases where the observed spectral radiance is greater than that possible for any 1D cloud, (2) cases where deviations from the ideal Nose Plot are too high for any 1D cloud and (3) the many cases where the rapid variation in spectral radiance is too high for 1D clouds.

9 Conclusions

Overall the good agreement between TWST and AERONET Cloud-Mode Cloud Optical Depths validates the performance of the Three Waveband Spectrally-agile Technique as well as the TWST sensor. Although the spectrally-agile nature of TWST was not investigated in this study, its advantage over fixed spectral bands for cases with high albedo at 440 nm will be the focus of a future study.

One of the most notable results of our experience with TWST is the high signal-to-noise ratio available in the high temporal (1 second), spatial (0.5 ° field of view), and spectral (2.5 nm) resolution data TWST generates. At peak signal, the SNR due to instrumental and photon noise is estimated to be 5,000:1. This peak occurs at a COD value of approximately OD 5, so the implied rms COD error is OD 0.001.

The version of the TWST algorithm used in this report was limited to use of the slope of the Nose Plot. This is mostly the result of limitations in our current ability to model the variation of EQW with COD, cloud base altitude, cloud average physical depth, cloud phase function, and solar zenith angle. If these effects can be normalized out, either from fitting to TWST measurements or to auxiliary measurements (lidar, radar, etc.), we expect that more accurate cloud states can be determined and, therefore, more accurate COD. In addition the values of the variables determined by fitting TWST data provide additional atmospheric information.

Acknowledgements

The authors thank Christine Chiu of University of Reading, UK for help in understanding the AERONET Cloud-Mode algorithm, Brent Holben and the AERONET team at NASA Goddard, Laurie Gregory and Richard Wegener of Brookhaven National Lab and Ilya Slutsker of Sigma Space Corp. for details on the particular AERONET sensor used at TCAP, as well as the TCAP PI Larry Berg of PNNL and Paul Ortega of LANL for permission to participate in TCAP, MAGIC PI Ernie Lewis of Brookhaven National Lab for the idea of a TWST deployment at TCAP, and Vaughan Ivens for invaluable assistance onsite at Cape Cod. Data were obtained from the Atmospheric Radiation Measurement (ARM) Program Climate Research Facility sponsored by the U.S. Department of Energy, Office of Science, Office of Biological and Environmental Research, Climate and Environment Sciences Division. The Cimel Sun-photometer data were collected by the U.S. Department of Energy as part of the Atmospheric Radiation Measurement (ARM) Program Climate Research Facility and processed by the National Aeronautics and Space Administration's Aerosol Robotic Network (AERONET).

References

Baldridge, A. M., Hook, S. J., Grove, C. I., and Rivera, G.: The ASTER Spectral Library Version 2.0., Remote Sens. Environ., 113, 711-715, 2009.

Barker, H. W., and Marshak, A.: Inferring optical depth of broken clouds above green vegetation using surface solar radiometric measurements, J. Atmos. Sci., 58, 2989-3006, 2001.

Berk, A., Anderson, G. P., Acharya, P. K., Bernstein, L. S., Muratov, L., Lee, J., Fox, M., Adler-Golden, S. M., Chetwynd, J. H., Hoke, M. L., Lockwood, R. B., Gardner, J. A., Cooley,

T. W., Borel, C. C., Lewis, P. E., and Shettle, E. P.: MODTRAN5: 2006 update, P. Soc. Photo-Opt. Ins., 6233, 62331F, 2006.

Chiu, J. C., Marshak, A., Knyazikhin, Y., Wiscombe, W., Barker, H., Barnard, J. C., and Luo, Y.: Remote sensing of cloud properties using ground-based measurements of zenith radiance, J. Geophys. Res. 111, D162011, doi:10.1029/2005JD006843, 2006.

Chiu, J. C., Huang, C.-H., Marshak, A., Slutsker, I., Giles, D. M., Holben, B. N., Knyazikhin, Y., and Wiscombe, W. J.: Cloud optical depth retrievals from the Aerosol Robotic Network (AERONET) cloud mode operation, J. Geophy. Res., 115, D14202, doi:10.1029/2009JD013121, 2010.

Chiu, J. C., Marshak, A., Huang, C.-H., Várnai, T., Hogan, R. J., Giles, D. M., Holben, B. N., O'Connor, E. J., Knyazikhin, Y., and Wiscombe, W. J.: Cloud droplet size and liquid water path retrievals from zenith radiance measurements: Examples from the Atmospheric Radiation Measurement Program and the Aerosol Robotic Network, Atmospheric Chemistry and Physics Discussions, 12:8, 19163–208, doi:10.5194/acpd-12-19163-2012, 2012.

Harrison, I. and Min, Q.-L.: Photon pathlength distributions in cloudy atmospheres from ground-based high-resolution O2 A-band spectroscopy. IRS'96 Current Problems in Atmospheric Radiation, W. L. Smith and K. Stamnes, Eds., Deepak Publishers, 594-597, 1997.

Marshak, A., Knyazikhin, Y., Davis, A., Wiscombe, W., and Pilewskie P.: Cloud-vegetation interaction. Use of normalized difference cloud index for estimation of cloud optical thickness, Geophys. Res. Lett., 27, 1695-1698, 2000.

Marshak, A., Knyazikhin, Y., Evans, K. D., and Wiscombe, W. J.: The "RED versus NIR" plane to retrieve broken-cloud optical depth from ground-based measurements, J. Atmos. Sci., 61, 1911-1925, 2004.

Mulliken, R. S.: Interpretation of the atmospheric oxygen bands; electronic levels of the oxygen molecule, Nature, 122, 505, 1928.

Pfeilsticker, K., Erle, F., Funk, O., Veitel, H., and Platt, U.: First geometrical pathlengths probability density function derivation of the skylight from spectroscopically highly resolving oxygen A-band observations, J. Geophys. Res., 103:D10, 11483-11504, 1998.

Pfeilsticker, K., Erle, F., Funk, O., Veitel, H., and Platt, U.: Cloudy sky photon pathlength as derived from DOAS-observations, IRS'96 Conference, Fairbanks, AK, 19-24 August 1996, 1996.

Stamnes, K., Tsay, S.-C., Wiscombe, W., and Jayaweera, K.: Numerically stable algorithm for discrete-ordinate-method radiative transfer in multiple scattering and emitting layered media, Appl. Optics, 27:12, 2502–9. doi:10.1364/AO.27.002502, 1988.

Stephens, G. L.: Radiation profiles in extended water clouds. II: Parameterization schemes, J. Atmos. Sci., 35:11, 2123–32, doi:10.1175/1520-0469(1978)035<2123:RPIEWC>2.0.CO;2, 1978.

Wark, D. Q. and Mercer, D. M.: Absorption in the atmosphere by the oxygen A band, Appl. Optics, 4, 839-844, 1965.

Wood, R., and Hartmann, D. L.: Spatial variability of liquid water path in marine low cloud: The importance of mesoscale cellular convection, J. Climate, 19:9, 1748–64. doi:10.1175/JCLI3702.1, 2006.

Atmos. Meas. Tech. Discuss., doi:10.5194/amt-2016-67, 2016
Manuscript under review for journal Atmos. Meas. Tech.
Published: 8 March 2016

Atmospheric Measurement Techniques Discussions

1 Table 1 TWST Cloud Optical Depth Sensor Specifications

2

TWST Cloud OD Sensor Specifications **For Ambient Temperature Range -10ºC to +40ºC**	
Weight	20 lbs
Power and Communication for Optical Head	5 Vdc, <250 mA via a single USB 2.0 cable connection to computer for power and data
Size	11 x 8 x 8 in plus 12 in external sun baffle; or 13 x 10 x 6 in with internal sun baffle
Operating Range	Blue Sky to Cloud OD 100
Cloud OD Sensitivity	0.001 for Optically Thin Clouds
Weatherproof Environmental Container	IP66, NEMA 4X sealed enclosure with desiccant
Data Logging Rate	1 Hz (typical), variable sampling interval from 0.1 to 60 seconds
Field of View	0.5 °
Spectral Range, Resolution	350 – 1000 nm, ~2.5 nm
Spectral Bands currently used in Cloud OD retrieval	440, 760, and 870 nm

Atmos. Meas. Tech. Discuss., doi:10.5194/amt-2016-67, 2016
Manuscript under review for journal Atmos. Meas. Tech.
Published: 8 March 2016

Atmospheric Measurement Techniques Discussions

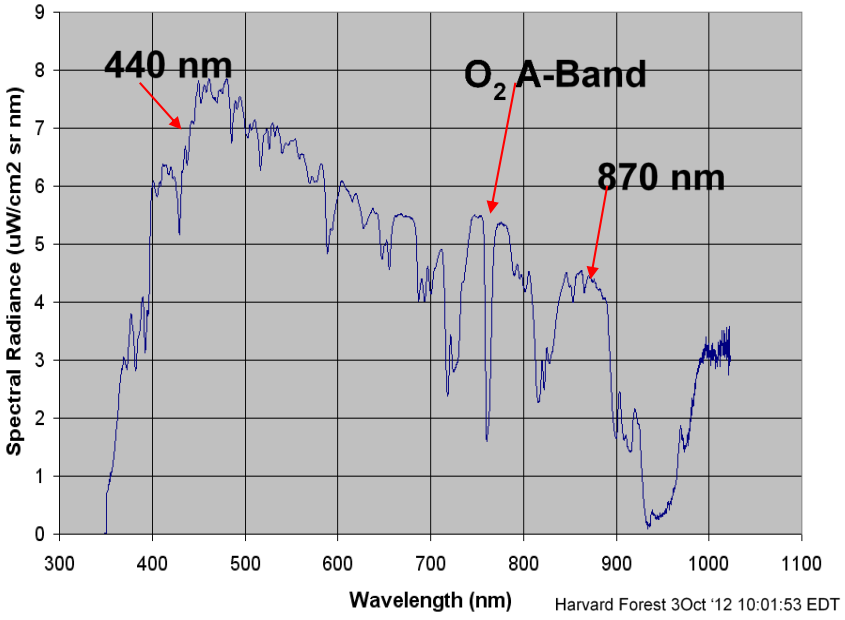

1

2 Figure 1. The three spectral factors currently used in TWST.

3

Atmos. Meas. Tech. Discuss., doi:10.5194/amt-2016-67, 2016
Manuscript under review for journal Atmos. Meas. Tech.
Published: 8 March 2016

Atmospheric Measurement Techniques Discussions

1

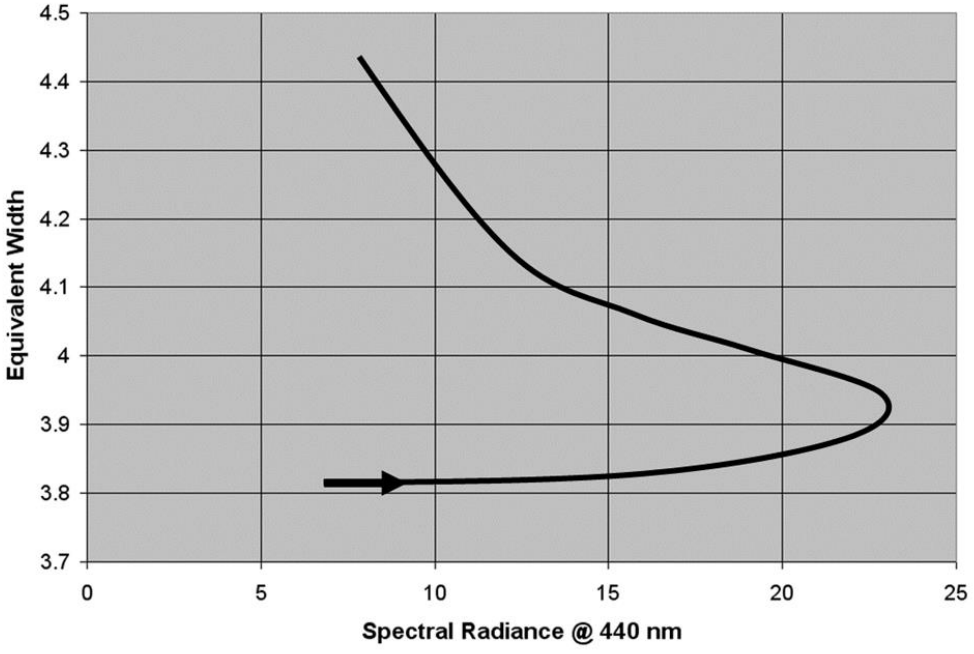

2

3 Figure 2. The “nose” plot, indicating a trajectory with increasing COD.

4

Atmos. Meas. Tech. Discuss., doi:10.5194/amt-2016-67, 2016
Manuscript under review for journal Atmos. Meas. Tech.
Published: 8 March 2016

Atmospheric Measurement Techniques Discussions

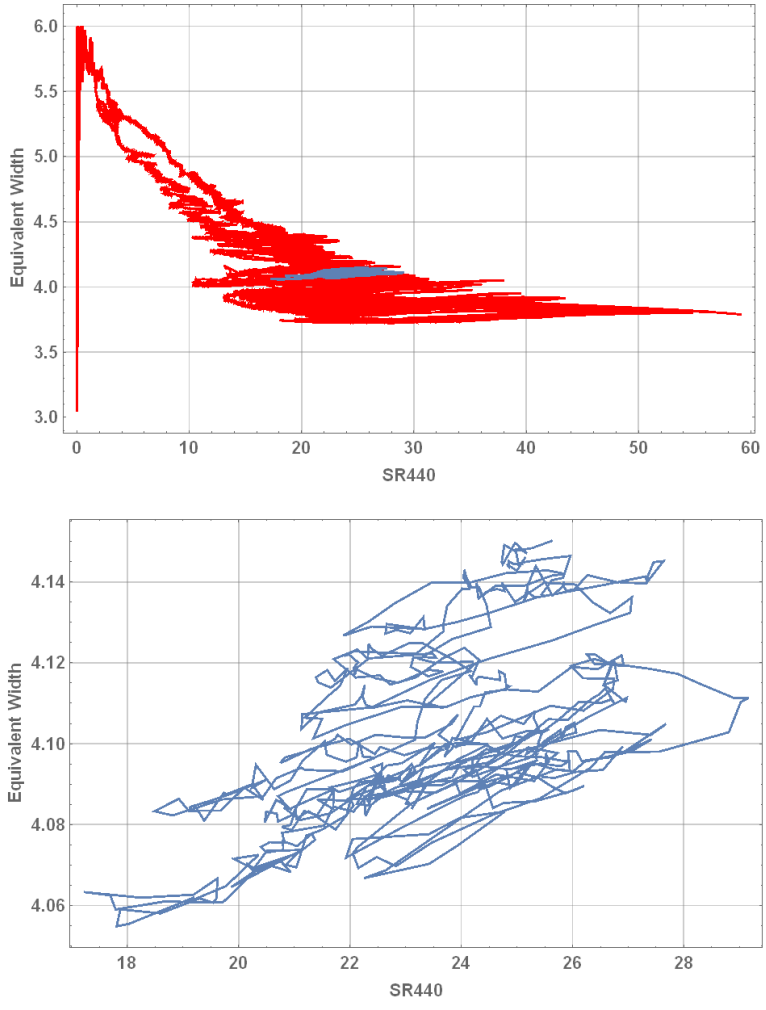

1

2 Figure 3. Measured nose plots. (Top) Over 13 hours of continuous data with a 10 minute
3 segment indicated in blue. (Bottom) Zoomed plot of 10 minute segment.

4

Atmos. Meas. Tech. Discuss., doi:10.5194/amt-2016-67, 2016
Manuscript under review for journal Atmos. Meas. Tech.
Published: 8 March 2016

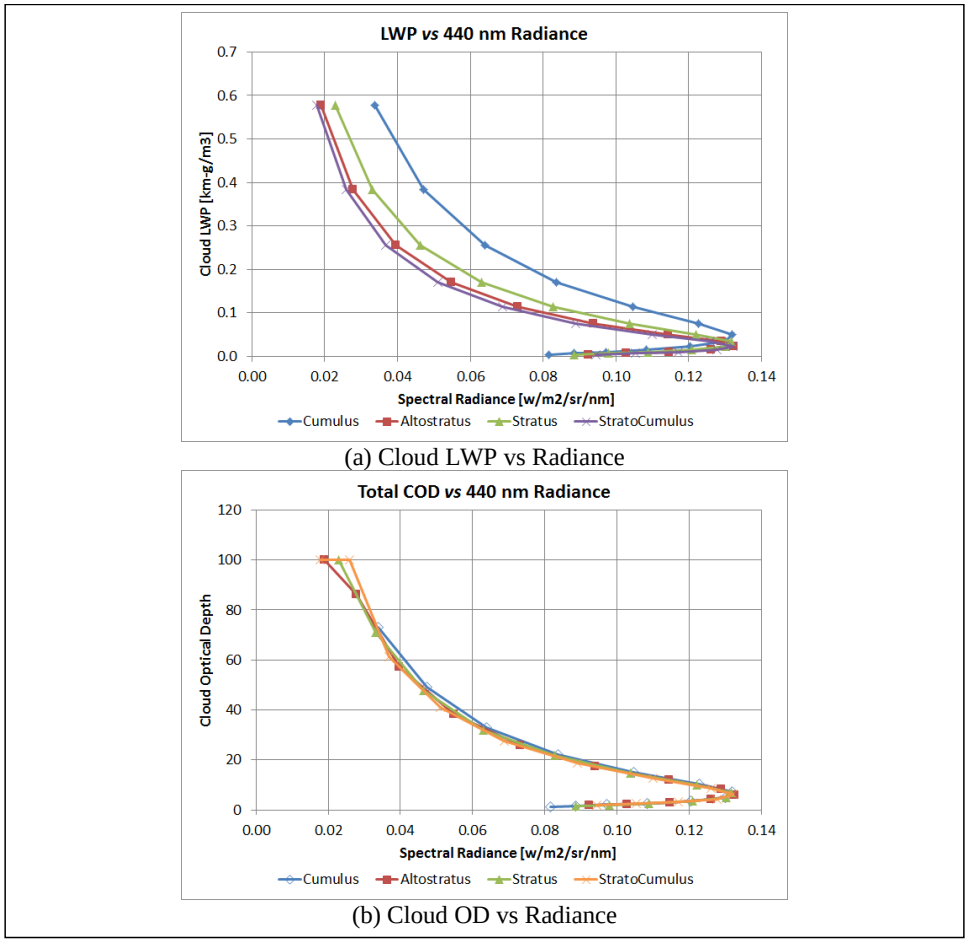

(a) Cloud LWP vs Radiance

(b) Cloud OD vs Radiance

Figure 4. Relationship between Spectral Radiance at 440 nm wavelength and a) liquid water path and b) cloud optical depth for four different cloud types.

Atmos. Meas. Tech. Discuss., doi:10.5194/amt-2016-67, 2016
Manuscript under review for journal Atmos. Meas. Tech.
Published: 8 March 2016

Atmospheric Measurement Techniques Discussions

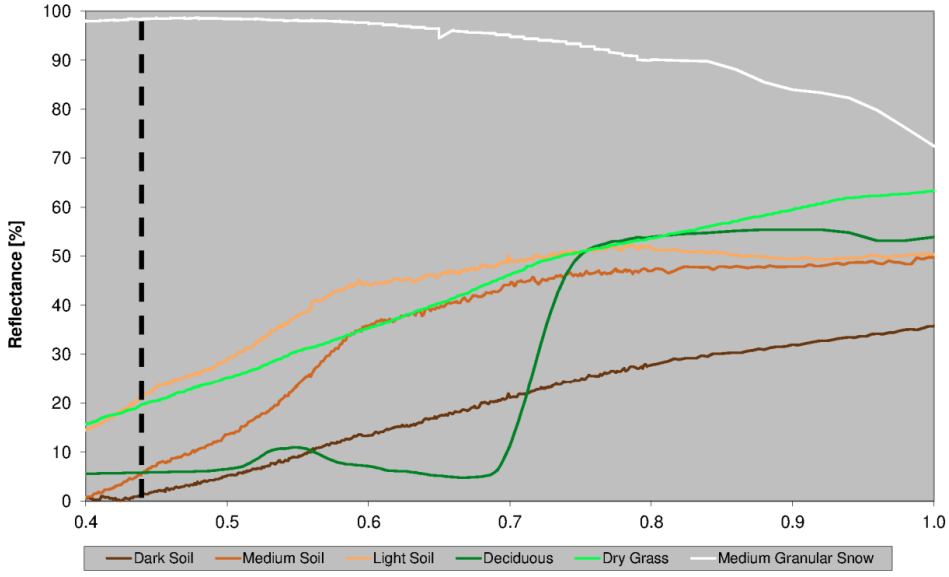

1

2 Figure 5. Spectral albedos of common Earth cover types from the ASTER Database; the
3 vertical dashed line indicates 440nm wavelength.

4

Atmos. Meas. Tech. Discuss., doi:10.5194/amt-2016-67, 2016
Manuscript under review for journal Atmos. Meas. Tech.
Published: 8 March 2016

Atmospheric Measurement Techniques Discussions

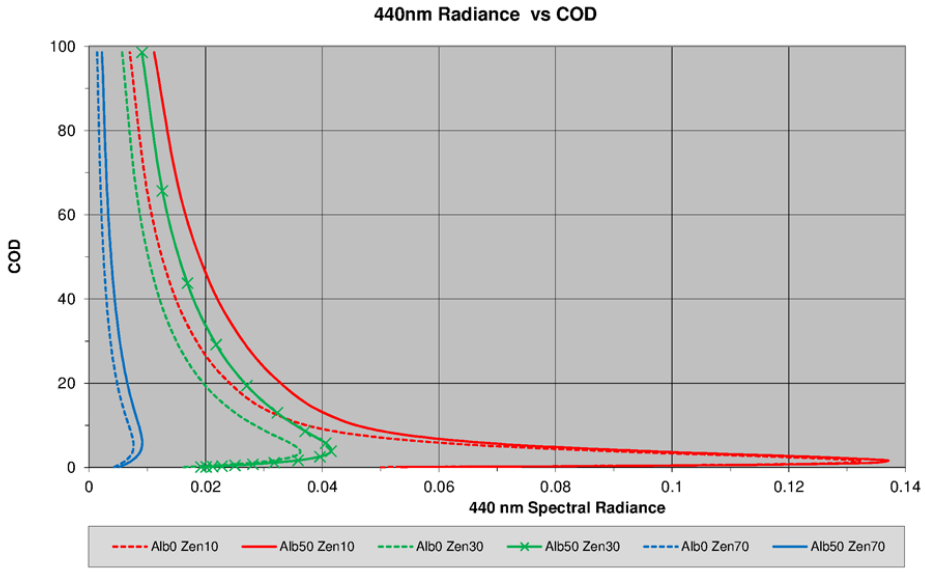

1

2 Figure 6. Cloud OD vs 440 nm radiance (w m^{-2} sr^{-1} nm^{-1}) for solar zeniths of 10, 30 and 70
3 deg and for albedos of 0.0 (dashed lines) and 0.50 (solid lines).

4

Atmos. Meas. Tech. Discuss., doi:10.5194/amt-2016-67, 2016
Manuscript under review for journal Atmos. Meas. Tech.
Published: 8 March 2016

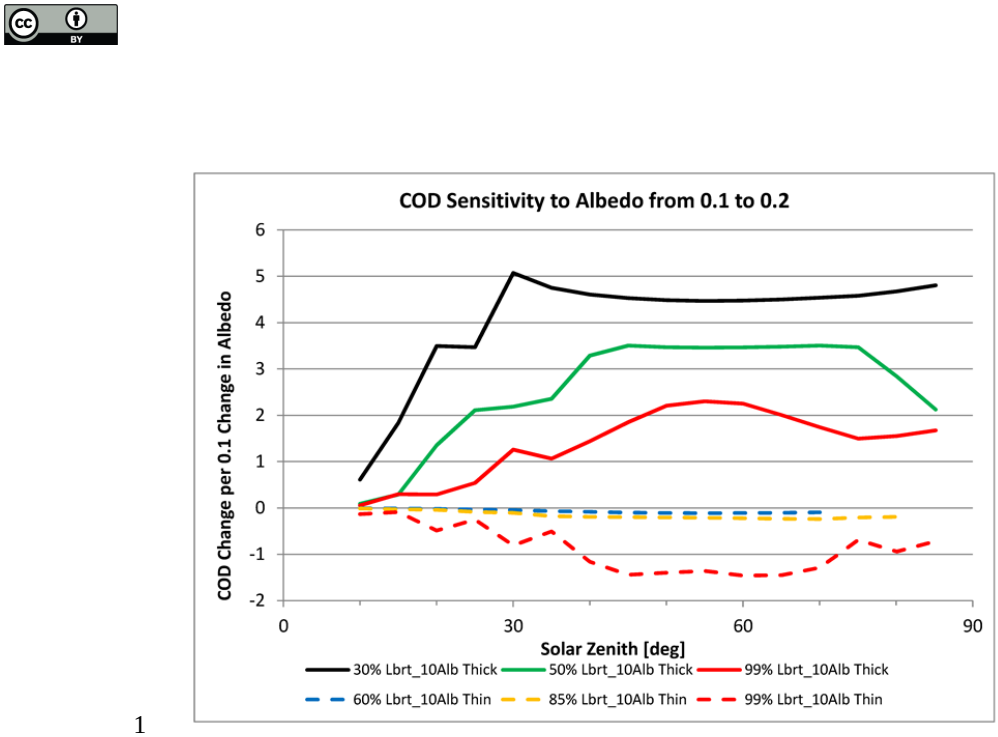

Figure 7. COD sensitivity to change in albedo from 0.1 to 0.2 for different relative cloud radiance levels (percent of the SZA-dependent bright point radiance Lbrt).

Atmos. Meas. Tech. Discuss., doi:10.5194/amt-2016-67, 2016
Manuscript under review for journal Atmos. Meas. Tech.
Published: 8 March 2016

Atmospheric Measurement Techniques Discussions

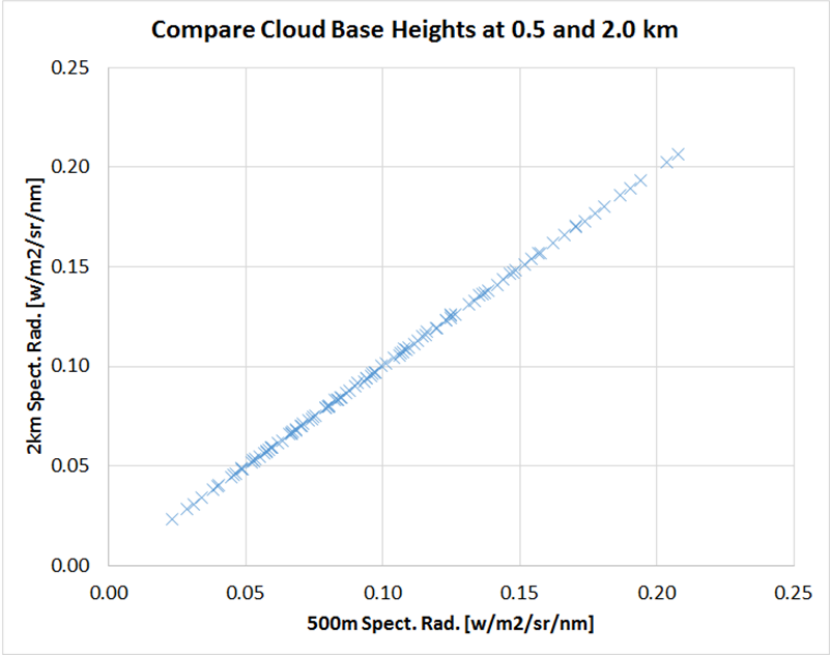

Figure 8. Scatter plot comparing 440 nm radiance computed for cloud base heights of 500 m and 2 km, each varying over 10 COD and 11 solar zenith angles.

Atmos. Meas. Tech. Discuss., doi:10.5194/amt-2016-67, 2016
Manuscript under review for journal Atmos. Meas. Tech.
Published: 8 March 2016

Atmospheric Measurement Techniques Discussions

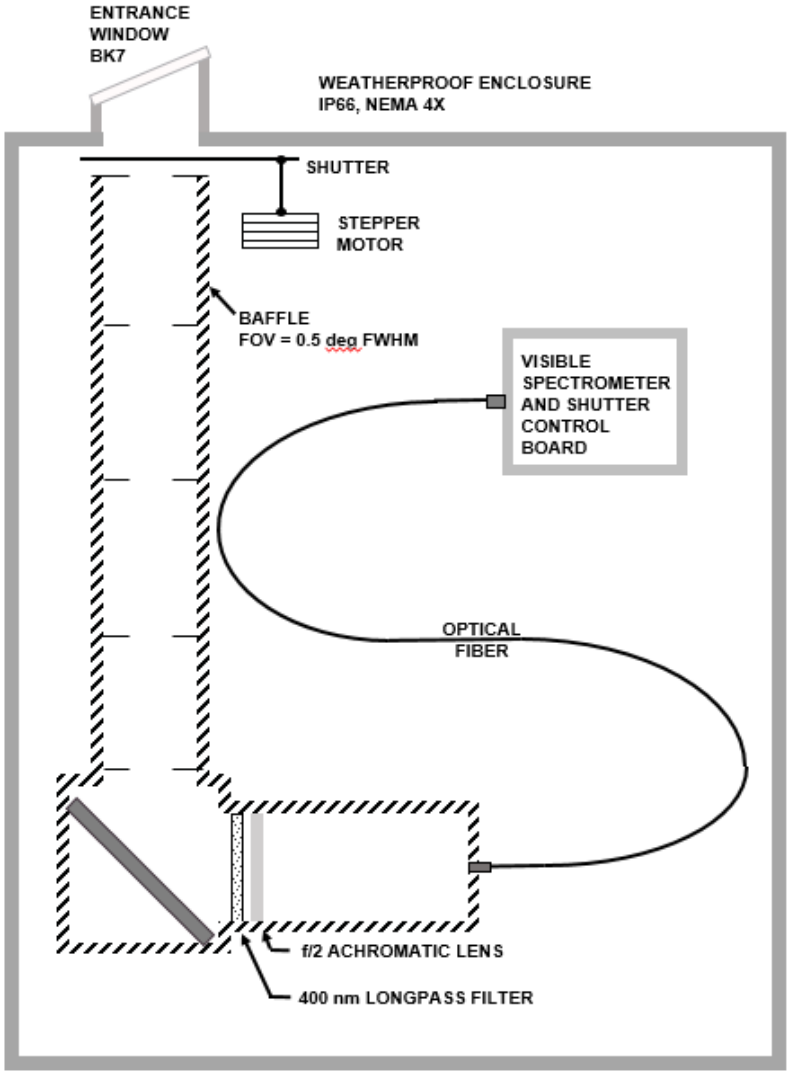

Figure 9 Simplified Schematic of the TWST Cloud Optical Depth Sensor.

Atmos. Meas. Tech. Discuss., doi:10.5194/amt-2016-67, 2016
Manuscript under review for journal Atmos. Meas. Tech.
Published: 8 March 2016

Atmospheric Measurement Techniques Discussions

1

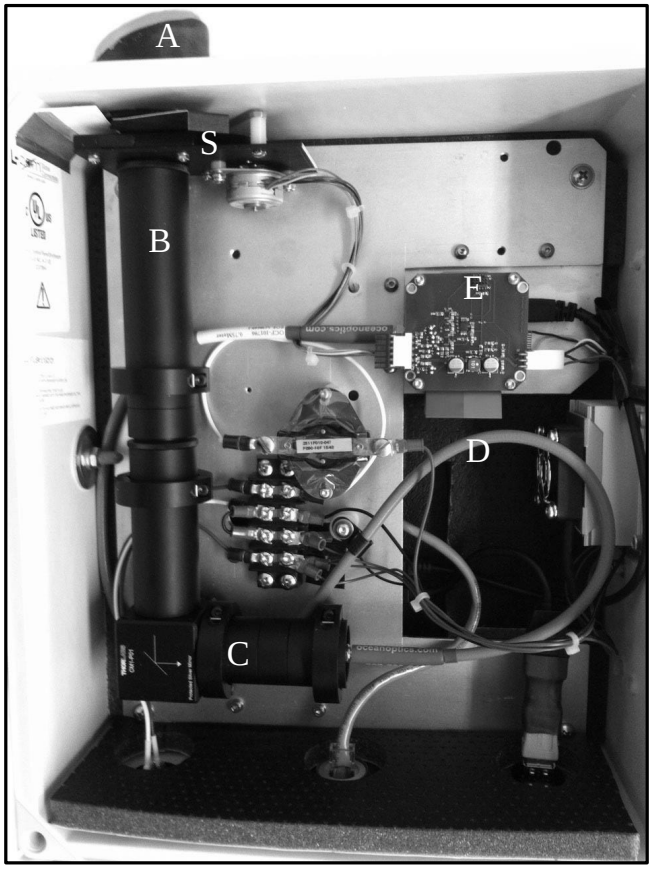

2
3
4 Figure 10 A look inside the TWST Cloud Optical Depth Sensor

5

Atmos. Meas. Tech. Discuss., doi:10.5194/amt-2016-67, 2016
Manuscript under review for journal Atmos. Meas. Tech.
Published: 8 March 2016

1

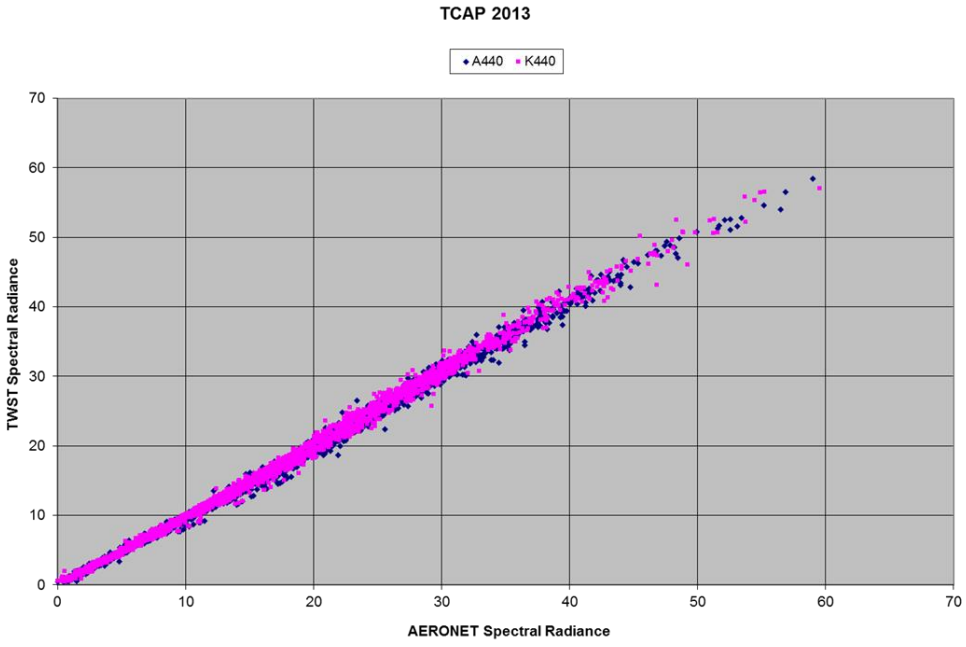

2

3 Figure 11. Comparison of TWST and AERONET Cloud-Mode spectral radiances (μW cm^{-2}
4 sr^{-1} nm^{-1}) at 440 nm wavelength.

Atmos. Meas. Tech. Discuss., doi:10.5194/amt-2016-67, 2016
Manuscript under review for journal Atmos. Meas. Tech.
Published: 8 March 2016

Atmospheric Measurement Techniques Discussions

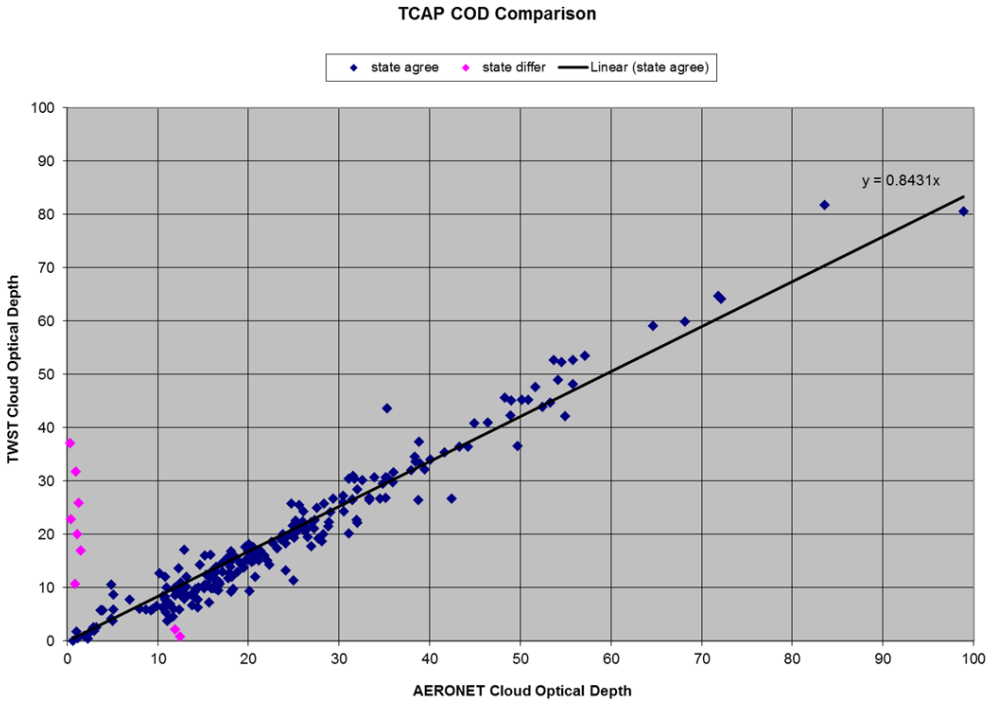

Figure 12 Comparison of TWST and AERONET Cloud-Mode Cloud Optical Depths.